Decentralized Filters for the Formation Flight

Eun-Jung Song*
Department of Mechanical and Aerospace Engineering
University of California, Los Angeles, Los Angeles, California 90095-1597 U.S.A.

Abstract

Decentralized filtering for a formation flight instrumentation system by INS/GPS integration is considered in this paper. An elaborate tuning method of the measurement noise covariance is suggested to compensate modeling errors caused by decentralizing the extended Kalman filter. It does not require large data transfer between formation vehicles. Covariance analysis exhibits the superior performance of the proposed approach when compared with the existent decentralized filter and the global filter, which has the target-filter performance.

Key Word : formation flight, decentralized filtering, global filtering, covariance analysis

Introduction

The objective of the formation flight is to obtain a fuel saving benefit, which results from the aerodynamic drag reduction by flying multiple aircraft in formation [1, 2]. Also, replacing one traditional complex aircraft with several simpler aircraft improves flexibility and offers a high degree of redundancy and reconfigurability in the event of a vehicle failure. For the tight maintenance and control of the formation, the navigation system must provide high accurate estimates of the relative position, velocity, and attitudes in real time to each aircraft control system. High accuracy is required for each aircraft to be precisely located at the position where the drag can be reduced most.

UCLA (University of California, Los Angeles) is building and testing an instrumentation package for the formation flight, which is sponsored by NASA DFRC (Dryden Flight Research Center) and Boeing. A GPS (Global Positioning System) receiver and a strap-down IMU (Inertial Measurement Unit) are employed on each aircraft as the primary instruments for navigation. The GPS provides an accurate set of measurements for online calibration of the IMU while the IMU provides its measurements at a higher rate than the GPS measurements. Several researches have been performed in the area of navigation using GPS/INS [3-10]. Most of them employ the EKF (Extended Kalman Filter) as a GPS/INS fusion algorithm and require extensive ground supports for computation. However to conduct the formation flight autonomously without extensive ground support, it is essential to develop a decentralized filtering algorithm for each aircraft, which requires less computation and transmission loads with the least loss of the global (central) filtering performance.

For this purpose, UCLA had developed a decentralized EKF algorithm, which requires equal computational loads between formation vehicles [9]. However it does not consider the modeling error caused by the lever-arm vector (the vector from the IMU to the antenna) difference between formation vehicles. In this article, a new tuning method for the decentralized filter in Ref. [9] is suggested to compensate the error by the elaborate choice of the filter design parameter R, the measurement noise covariance of the decentralized EKF. All data collected by GPS systems are referenced to the antenna location, namely the phase center of the antenna. However in most applications the goal

* Post-Doc.
E-mail : ejsong@viva.kari.re.kr, TEL : 042-860-2994, FAX : 042-860-2233

is to position the IMU at the center of mass of the aircraft, not the location of the antenna distant from the IMU. Therefore the GPS data collected must be transformed to the IMU location. This is done by accurately measuring and recording the lever-arm vector. The incorrectly measured or recorded lever-arm vector is one of the primary error sources encountered when performing any type of GPS usage [11]. Furthermore the lever-arm vector difference among formation-flight vehicles induces some modeling errors, which degrades the filter-performance.

Another attractive aspect of this approach is that it permits a direct trade between estimation accuracy and computational load. Covariance analysis shows a promising result in that it produces similar performance of the global filtering as well as provides a more accuracy than the decentralized filter in Ref. [9].

Some other results and perspectives of decentralized filtering have been presented in Ref. [12-17]. The unifying motivation of these approaches is the need to develop distributed or parallel implementation of well-known estimation algorithms such as the Kalman filter. Early theoretical approaches developed in Ref. [12-15] are generally not suitable or practical for real-time estimation due to significant data transfer requirements. Carlson developed an efficient federated Kalman filter for use in distributed multisensor systems [16]. However he did not consider the case when the measurement noise processes are correlated in different sensors like the common-mode noises of several GPS receivers. Ref. [17] presented a necessary and sufficient condition for optimality of the decentralized estimator in the presence of correlated measurement noise processes. However they considered only the static estimation problem since that in itself illustrates the obstacles to achieving optimality.

This paper is organized as follows: The navigation error modeling of IMU aided by GPS is described first. The existent approaches of decentralized filtering and new augmented decentralized filtering suggested in this paper are then explained. Next, covariance analysis is performed to investigate the performance of the proposed scheme. Finally, the conclusions of this work is summarized.

Navigation Error Modeling

The nonlinear navigation equations in the ECEF (Earth Centered and Earth Fixed) frame are given by [18]

$$\dot{P} = V \tag{1}$$

$$\dot{V} = C_B^E f^b - 2\Omega_{ie}^e V + g^e \tag{2}$$

$$\dot{C}_B^E = C_B^E \Omega_{eb}^b \tag{3}$$

where P is the position and V the velocity in the ECEF frame, f^b is the specific force vector in the body frame, C_B^E is the direction cosine matrix from the body frame to the ECEF frame, $\Omega_{ie}^e (\equiv [\omega_{ie}^e \times])$ is the skew-symmetric cross product matrix of the Earth rotational velocity ω_{ie}^e, g^e is the gravity vector in the ECEF frame, and $\Omega_{eb}^b = [\omega_{eb}^b \times]$, the angular velocity of the body frame relative to the ECEF frame represented in the body frame.

The pseudorange measurement of the jth GPS antenna to the ith satellite is given by

$$\widetilde{r_{G-S}^{(i,j)}} = |P_G^{(j)} - P_S^{(i)}| + ct + \eta^r \tag{4}$$

where $P_G^{(j)}$ denotes the jth antenna position in the ECEF frame, $P_S^{(i)}$ denotes the ith satellite position in the ECEF frame, ct is the receiver clock bias (c is the speed of light), and η^r is the statistical error. Here a single multiantenna receiver system is employed for simplicity. The pseudorange rate measurement to the ith satellite is

$$\widetilde{\dot{r}_{G-S}^{(i,j)}} = \frac{(P_G^{(j)} - P_S^{(i)}) \cdot (V_G^{(j)} - V_S^{(i)})}{|P_G^{(j)} - P_S^{(i)}|} + c\dot{t} + \eta^{\dot{r}} \tag{5}$$

where $V_G^{(j)}$ and $V_S^{(i)}$ denote the antenna velocity and the satellite velocity in the ECEF frame, respectively, $c\dot{t}$ is the drift of the receiver clock bias, and η^{r} is the statistical error. The relationship between the IMU position and the jth antenna is given by

$$P_G^{(j)} = P + C_B^E l^{(j)} \tag{6}$$

where $l^{(j)}$ denotes the lever-arm vector from the IMU to the jth antenna in the body frame. In the velocity case,

$$V_G^{(j)} = V + \omega_{eb}^e \times C_B^E l^{(j)} \tag{7}$$

Using Eqs. (1) through (7), the following linear error equations are obtained by the standard procedure of their derivation [19]:

$$\frac{d}{dt}\begin{bmatrix} \delta P \\ \delta V \\ \psi \\ b^g \\ b^a \\ c\delta t \\ c\delta \dot{t} \end{bmatrix} = \begin{bmatrix} 0_{3\times3} & I_{3\times3} & 0_{3\times3} & 0_{3\times3} & 0_{3\times3} & 0_{9\times2} \\ G & -2\Omega_{ie}^e & [C_B^E f^b\times] & 0_{3\times3} & C_B^E & \\ 0_{3\times3} & 0_{3\times3} & -\Omega_{ie}^e & -C_B^E & 0_{3\times3} & \\ 0_{6\times15} & & & & & 0_{6\times2} \\ & & & & & \\ 0_{2\times15} & & & & & \begin{matrix} 0 & 1 \\ 0 & 0 \end{matrix} \end{bmatrix} \begin{bmatrix} \delta P \\ \delta V \\ \psi \\ b^g \\ b^a \\ c\delta t \\ c\delta \dot{t} \end{bmatrix} + \begin{bmatrix} 0_{3\times1} \\ 0_{3\times1} \\ 0_{3\times1} \\ w^g \\ w^a \\ 0 \\ w^{\dot{t}} \end{bmatrix} \tag{8}$$

where ψ represents the attitude errors, b^g and b^a represent the gyro and the accelerometer biases, respectively, G is the gravity gradient, and $w^{(\cdot)}$ denotes the process noise. For the ith satellite, in the code measurement of the jth antenna case,

$$H^{\rho(i,j)} = \begin{bmatrix} \dfrac{(P_G^{(j)} - P_S^{(i)})^T}{|P_G^{(j)} - P_S^{(i)}|} & 1 \end{bmatrix} \begin{bmatrix} I_{3\times3} & 0_{3\times3} & [C_B^E l^{(j)}\times] & 0_{3\times3} & 0_{3\times3} & 0_{3\times1} & 0_{3\times1} \\ 0_{1\times3} & 0_{1\times3} & 0_{1\times3} & 0_{1\times3} & 0_{1\times3} & 1 & 0 \end{bmatrix} \tag{9}$$

In the doppler measurement case,

$$H^{\dot{\rho}(i,j)} = \begin{bmatrix} \dfrac{(P_G^{(j)} - P_S^{(i)})^T}{|P_G^{(j)} - P_S^{(i)}|} & 1 \end{bmatrix} \times \begin{bmatrix} 0_{3\times3} & I_{3\times3} & [C_B^E(\omega_{ib}^b \times l^{(j)})\times] - \Omega_{ie}^e[C_B^E l^{(j)}\times] & -C_B^E[l^{(j)}\times] & 0_{3\times3} & 0_{3\times1} & 0_{3\times1} \\ 0_{1\times3} & 0_{1\times3} & 0_{1\times3} & 0_{1\times3} & 0_{1\times3} & 0 & 1 \end{bmatrix} \tag{10}$$

Decentralized Filtering

1. Global formation flight system

The formation flight with two aircraft is considered here. The problem can be equally extended to the n multiple-aircraft formation case. One aircraft will be called *base vehicle*, and the other will be called *slave vehicle*. Each aircraft has one IMU and one GPS receiver. Then the nonlinear navigation processor for each vehicle is given by

$$\dot{\mathbf{x}}_b = \mathbf{f}_b(\mathbf{x}_b, t) \tag{11}$$

$$\dot{\mathbf{x}}_s = \mathbf{f}_s(\mathbf{x}_s, t) \tag{12}$$

where $(\cdot)_b$ and $(\cdot)_s$ denote the base vehicle states and the slave vehicle states, respectively. Eqs. (1) through (3) show the detailed description of Eqs. (11) and (12). The linearized model for this system is

$$\begin{bmatrix} \delta\dot{\mathbf{x}}_s \\ \delta\dot{\mathbf{x}}_b \end{bmatrix} = \begin{bmatrix} A_s & 0 \\ 0 & A_b \end{bmatrix} \begin{bmatrix} \delta\mathbf{x}_s \\ \delta\mathbf{x}_b \end{bmatrix} + \begin{bmatrix} \mathbf{w}_s \\ \mathbf{w}_b \end{bmatrix} \tag{13}$$

$$\begin{bmatrix} \rho_s - \overline{\rho_s} \\ \rho_b - \overline{\rho_b} \end{bmatrix} = \begin{bmatrix} H_s & 0 \\ 0 & H_b \end{bmatrix} \begin{bmatrix} \delta x_s \\ \delta x_b \end{bmatrix} + \begin{bmatrix} v_s + b_c \\ v_b + b_c \end{bmatrix} \tag{14}$$

Eqs. (8) through (10) show the detailed description. The EKF processing of Eqs. (13) and (14) in one aircraft to consider the common-mode noises b_c of the GPS measurements requires heavy computational burden and communication load between vehicles ($v_{(\cdot)}$ denotes the noncommon-mode noises of the GPS measurements). The correlation of the GPS measurements noise processes between vehicles makes the decomposition of the equations be difficult.

2. Existent decentralized filter I

Williamson, *et al.* [9] suggested the following decentralized filtering to solve the problem in Sec. 1. The linearized global dynamics are transformed to cancel the common-mode noises:

$$\begin{aligned} \begin{bmatrix} \delta \dot{x}_b \\ \Delta \delta \dot{x} \end{bmatrix} &= \begin{bmatrix} A_b & 0 \\ A_s - A_b & A_s \end{bmatrix} \begin{bmatrix} \delta x_b \\ \Delta \delta x \end{bmatrix} + \begin{bmatrix} w_b \\ w_s - w_b \end{bmatrix} \\ &= \begin{bmatrix} A_b & 0 \\ \Delta A & A_s \end{bmatrix} \begin{bmatrix} \delta x_b \\ \Delta \delta x \end{bmatrix} + \begin{bmatrix} w_b \\ \Delta w \end{bmatrix} \end{aligned} \tag{15}$$

$$\begin{aligned} \begin{bmatrix} \rho_b \\ \Delta \rho \end{bmatrix} &= \begin{bmatrix} \overline{\rho_b} \\ \Delta \overline{\rho} \end{bmatrix} + \begin{bmatrix} H_b & 0 \\ H_s - H_b & H_s \end{bmatrix} \begin{bmatrix} \delta x_b \\ \Delta \delta x \end{bmatrix} + \begin{bmatrix} v_b + b_c \\ v_s - v_b \end{bmatrix} \\ &= \begin{bmatrix} \overline{\rho_b} \\ \Delta \overline{\rho} \end{bmatrix} + \begin{bmatrix} H_b & 0 \\ \Delta H & H_s \end{bmatrix} \begin{bmatrix} \delta x_b \\ \Delta \delta x \end{bmatrix} + \begin{bmatrix} v_b + b_c \\ \Delta v \end{bmatrix} \end{aligned} \tag{16}$$

where $\Delta = (\cdot)_s - (\cdot)_b$. If two vehicles fly along similar trajectories,

$$\Delta A \approx 0 \tag{17}$$

$$\Delta H \approx 0 \tag{18}$$

Using the approximations in Eqs. (17) and (18), Eqs. (15) and (16) can be decomposed as follows:

$$\begin{aligned} \text{Base vehicle:} \quad \delta \dot{x}_b &\approx A_b \delta x_b + w_b \\ \rho_b - \overline{\rho_b} &\approx H_b \delta x_b + v_b + b_c \end{aligned} \tag{19}$$

$$\begin{aligned} \text{Slave vehicle:} \quad \Delta \delta \dot{x} &\approx A_s \Delta \delta x + \Delta w \\ \Delta \rho - \Delta \overline{\rho} &\approx H_s \Delta \delta x + \Delta v \end{aligned} \tag{20}$$

Although the process noises are correlated by the new construction (the accurate IMU measurements might reduce the correlation), the correlation of the measurements is significantly reduced since the uncommon-mode noise errors are much smaller than the common-mode errors, especially, in the carrier phase measurements.

Now the implementation of each aircraft is independent. However if two vehicles experience the situation where the approximations in Eqs. (17) and (18) are not valid, the performance of the decentralized filter in Eqs. (19) and (20) might be degenerate. The difference between the lever-arm vectors of two vehicles can induce the situation, as can be seen in Eqs. (9) and (10).

3. Existent decentralized filter II

Ref. [9] suggested another decentralized filter as follows:

$$\begin{aligned} \text{Base vehicle:} \quad \delta \dot{x}_b &= A_b \delta x_b + w_b \\ \rho_b - \overline{\rho_b} &= H_b \delta x_b + v_b + b_c \end{aligned} \tag{21}$$

$$\begin{aligned} \text{Slave vehicle:} \quad \delta \dot{x}_s &= A_s \delta x_s + w_s \\ \rho_s - \overline{\rho_s} &= H_s \delta x_s + v_s + b_c \end{aligned} \tag{22}$$

The decentralized filters do ignore some potentially usable system information, knowledge of common-mode noises. The filter gain K^o for the global system in Eqs. (13) and (14) is approximated in this filter as follows:

$$K^o \equiv \begin{bmatrix} K^o_{11} & K^o_{12} \\ K^o_{21} & K^o_{22} \end{bmatrix} \approx \begin{bmatrix} K^o_s & 0 \\ 0 & K^o_b \end{bmatrix} \tag{23}$$

From the following relationship between the original global dynamics in Eqs. (13) and (14) and the relative global dynamics in Eqs. (15) and (16)

$$\begin{bmatrix} \delta x_b \\ \Delta\delta x \end{bmatrix} = S_n \begin{bmatrix} \delta x_s \\ \delta x_b \end{bmatrix}, \quad \begin{bmatrix} \rho_b \\ \Delta\rho \end{bmatrix} = S_m \begin{bmatrix} \rho_s \\ \rho_b \end{bmatrix}, \quad S_k \equiv \begin{bmatrix} 0_{k\times k} & I_{k\times k} \\ I_{k\times k} & -I_{k\times k} \end{bmatrix} \tag{24}$$

where n denotes the number of states δx_b or $\Delta\delta x$, and m the number of measurements ρ_b or $\Delta\rho$. Then filter gain for the linearized relative global dynamics can be derived as follows:

$$K = S_n K^o S_m^{-1} = \begin{bmatrix} (K^o_{21}+K^o_{22}) & K^o_{21} \\ (K^o_{11}-K^o_{21}+K^o_{12}-K^o_{22}) & (K^o_{11}-K^o_{21}) \end{bmatrix} \tag{25}$$

$$\begin{aligned} \begin{bmatrix} \delta\hat{x}_b \\ \Delta\delta\hat{x} \end{bmatrix} &= \begin{bmatrix} (K^o_{21}+K^o_{22})(\rho_b - \overline{\rho_b}) + K^o_{21}(\Delta\rho - \Delta\overline{\rho}) \\ (K^o_{11}-K^o_{21}+K^o_{12}-K^o_{22})(\rho_b - \overline{\rho_b}) + (K^o_{11}-K^o_{21})(\Delta\rho - \Delta\overline{\rho}) \end{bmatrix} \\ &\approx \begin{bmatrix} K^o_b(\rho_b - \overline{\rho_b}) \\ (K^o_s - K^o_b)(\rho_b - \overline{\rho_b}) + K^o_s(\Delta\rho - \Delta\overline{\rho}) \end{bmatrix} \end{aligned} \tag{26}$$

It shows that K^o_s designed for the slave dynamics in Eq. (22), which includes large common-mode errors b_c, is used as the filter gain for the differential measurements $\Delta\rho$, which has much smaller noise covariance Δv. Therefore the approach might have worse performance than that described in Sec. 2.

The common-mode error states can be included in each vehicle dynamics to eliminate them. Then the problem to increase the accuracy of relative state estimates results in the problem to increase the accuracy of single vehicle state estimates. However their estimation accompanies with the increase of the size of the system and it is well known that the differential operation is more appropriate to remove them [20].

4. Augmented decentralized filter

In this paper, an ad-hoc approach to improve the decentralized filter in Sec. 2 is proposed. From Eq. (16),

$$\begin{aligned} \Delta\rho - \Delta\overline{\rho} &= \Delta H\, \delta x_b + H_s\, \Delta\delta x + \Delta v \\ &= H_s\, \Delta\delta x + (\Delta H\, \delta x_b + \Delta v), \end{aligned} \tag{27}$$

$$\begin{aligned} R_s^{aug} &\equiv E[(\Delta H\, \delta x_b + \Delta v)(\Delta H\, \delta x_b + \Delta v)^T] \\ &= \Delta H E[\delta x_b \delta x_b^T]\Delta H^T + \Delta H E[\delta x_b \Delta v^T] + E[\Delta v \delta x_b^T]\Delta H^T + E[\Delta v \Delta v^T] \\ &\approx \Delta H P_b^- \Delta H^T + R_s, \quad R_s \equiv E[\Delta v \Delta v^T] \end{aligned} \tag{28}$$

To consider the nonzero ΔH, the measurement noise covariance of the decentralized filter R_s is changed into R_s^{aug}. Note that R_s^{aug} becomes R_s when ΔH=0. So this value does not degrade the performance obtained when the approximation in Eq. (18) is valid. It will be superior to the simple method that the large value of R_s is always used. Afterward it will be called the *augmented decentralized filter*. To employ the proposed approach, the additional transmission of $\Delta H P_b^- \Delta H^T$ from the base vehicle to the slave vehicle is required.

By the symmetric property of the matrix $\Delta H P_b^- \Delta H^T$, it is needed to transmit only 21 variables for one GPS antenna whenever the GPS measurements are available:

$$\Delta H P_b^- \Delta H^T \approx H_{\text{LOS}_s} \Delta H_{\text{loose}} P_b^- \Delta H_{\text{loose}}^T H_{\text{LOS}_s}^T \tag{29}$$

where

$$\Delta H \approx H_{\text{LOS}_s} \Delta H_{\text{loose}}, \qquad H^{(i)}{}_{\text{LOS}_s} = \frac{(P_{G_s} - P_S^{(i)})^T}{|P_{G_s} - P_S^{(i)}|},$$

$$H_{\text{LOS}_s} = \begin{bmatrix} H^{(1)}_{\text{LOS}_s} & 0_{1\times 3} \\ 0_{1\times 3} & H^{(1)}_{\text{LOS}_s} \\ H^{(2)}_{\text{LOS}_s} & 0_{1\times 3} \\ 0_{1\times 3} & H^{(2)}_{\text{LOS}_s} \\ \cdots & \cdots \\ H^{(m)}_{\text{LOS}_s} & 0_{1\times 3} \\ 0_{1\times 3} & H^{(m)}_{\text{LOS}_s} \end{bmatrix}, \qquad \Delta H_{\text{loose}} = \begin{bmatrix} \Delta H^b_{\text{loose}} \\ \Delta H^v_{\text{loose}} \end{bmatrix},$$

$$\Delta H^b_{\text{loose}} = [0_{3\times 3} \; 0_{3\times 3} \; [C_B^E l\times]_s - [C_B^E l\times]_b \; 0_{3\times 3} \; 0_{3\times 3} \; 0_{3\times 1} \; 0_{3\times 1}],$$

$$\Delta H^v{}_{\text{loose}}^T = \begin{bmatrix} 0_{3\times 3} \\ 0_{3\times 3} \\ ([C_B^E(\omega^b_{ib}\times l)\times] - \Omega^e_{ie}[C_B^E l\times])_s - ([C_B^E(\omega^b_{ib}\times l)\times] - \Omega^e_{ie}[C_B^E l\times])_b \\ (-C_B^E[l\times])_s - (-C_B^E[l\times])_b \\ 0_{3\times 3} \\ 0_{3\times 1} \\ 0_{3\times 1} \end{bmatrix}$$

Here note that $\Delta H_{\text{loose}} P_b^- \Delta H_{\text{loose}}^T$ is a 6×6 symmetric matrix and is independent of the number of visible satellites.

Numerical Results

Covariance analysis

Covariance analysis [21, 22] is performed here to evaluate the decentralized EKFs described in the previous section. Although it is precluded as a complete analysis method to the EKF, the covariance analysis of a linearized Kalman filter provides an approximate analysis tool of the EKF. Here the global filtering model in Eqs. (15) and (16) corresponds to the assumed truth model and the decentralized model in Eqs. (19) and (20) corresponds to the design model. The performances of the decentralized filters described in Secs. 2 and 4 are compared with the target performance of the global filter.

Performance evaluation

The covariance test is carried out by defining two aircraft flight paths and simulated IMU measurements. The nominal trajectories flown by the two aircraft are almost straight. Both vehicles are affected by the turbulent air, where the turbulence intensity is that of the clear air $\sigma = 0.5$ m/s [23]. The different effect of turbulence on each aircraft makes the difference in their sensed measurements. This scenario is assumed to be one of the most typical formation flying situations. The IMU measurements are available at every 40 Hz. The aerodynamic effects of the formation flight such as the drag reduction of the trailing aircraft are ignored here for simplicity. Each aircraft has 3 GPS antennas which are not collocated from one another. During the flights, it is assumed that common 8 satellites are visible on each aircraft at every 2 Hz.

The process noise covariance Q and measurement noise covariance R of the decentralized filter in Sec. 2 (it will be called *decentralized filter* for simplicity) are chosen as [20]:

- base vehicle

$$Q_b = \begin{bmatrix} (1.75\times10^{-5})^2 I_{3\times3}\ (\text{rad/s})^2 & 0_{3\times3} & 0_{3\times1} \\ 0_{3\times3} & 0.001^2 I_{3\times3}\ (\text{m/s}^2)^2 & 0_{3\times1} \\ 0_{1\times3} & 0_{1\times3} & 10^{-8}\ (\text{m/s})^2 \end{bmatrix} \tag{30}$$

$$R_b^{\text{code}} = 62.47\ \text{m}^2 \tag{31}$$

$$R_b^{\text{doppler}} = 0.02\ (\text{m/s})^2 \tag{32}$$

- slave vehicle

$$Q_s = 2Q_b \tag{33}$$

$$R_s^{\text{single differenced code}} = 0.04\ \text{m}^2 \tag{34}$$

$$R_s^{\text{single differenced doppler}} = 0.0004\ (\text{m/s})^2 \tag{35}$$

From the relationship between the global system in Eqs. (15) and (16) and the decentralized system in Eqs. (19) and (20), those of the global filter are

$$Q = \begin{bmatrix} Q_b & -Q_b \\ -Q_b & Q_s \end{bmatrix}, \quad R = \begin{bmatrix} R_b & -\frac{R_s}{2} \\ -\frac{R_s}{2} & R_s \end{bmatrix} \tag{36}$$

The augmented decentralized filter uses the same Q_b and R_b in the base-vehicle case. On the other hand, Q_s and $R_s + \Delta H P_b \Delta H^T$ are employed in the slave-vehicle case as explained in Sec. 4. Then the covariance for each filter is computed by evaluating the partial derivative matrices A and H based on the nominal trajectories.

The comparison among the decentralized filter, the augmented decentralized filter, and the global filter are performed for the following two situations:

1. no lever-arm vector difference :

$$\begin{bmatrix} l_b^{(1)} \\ l_b^{(2)} \\ l_b^{(3)} \end{bmatrix} = \begin{bmatrix} l_s^{(1)} \\ l_s^{(2)} \\ l_s^{(3)} \end{bmatrix} = \begin{bmatrix} (6.00 & 0.00 & -1.00) \\ (0.00 & 1.00 & 0.00) \\ (0.00 & 0.00 & 1.00) \end{bmatrix} \quad (\text{m})$$

2. large lever-arm vector difference :

$$\begin{bmatrix} l_b^{(1)} \\ l_b^{(2)} \\ l_b^{(3)} \end{bmatrix} = \begin{bmatrix} (6.00 & 0.00 & -1.00) \\ (0.00 & 1.00 & 0.00) \\ (0.00 & 0.00 & 1.00) \end{bmatrix}, \quad \begin{bmatrix} l_s^{(1)} \\ l_s^{(2)} \\ l_s^{(3)} \end{bmatrix} = \begin{bmatrix} (7.14 & 1.00 & -1.14) \\ (0.37 & 1.14 & 0.00) \\ (0.00 & -0.37 & 1.14) \end{bmatrix} \quad (\text{m})$$

Table 1. Covariance analysis results

$\sqrt{P}$	Global	Decentralized	Augmented
$\Delta\delta x_E$ (cm)	2.5479	2.6730	2.7849
$\Delta\delta y_E$ (cm)	3.4272	3.9942	3.5752
$\Delta\delta z_E$ (cm)	2.1548	3.1674	2.1643
$\Delta\delta V_{x_E}$(cm/s)	0.4321	0.6387	0.6244
$\Delta\delta V_{y_E}$(cm/s)	0.4295	1.0890	0.8740
$\Delta\delta V_{z_E}$(cm/s)	0.4715	0.8375	0.5239
$\Delta\psi_1$ (deg)	0.0872	0.3415	0.2254
$\Delta\psi_2$ (deg)	0.1190	0.1835	0.2351
$\Delta\psi_3$ (deg)	0.1118	0.6702	0.3576

(a) no lever-arm vector difference

$\sqrt{P}$	Global	Decentralized	Augmented
$\Delta\delta x_E$ (cm)	2.5624	6.6702	2.8308
$\Delta\delta y_E$ (cm)	3.4359	5.9433	3.6398
$\Delta\delta z_E$ (cm)	2.1570	4.6129	2.1695
$\Delta\delta V_{x_E}$(cm/s)	0.4319	0.6113	0.6245
$\Delta\delta V_{y_E}$(cm/s)	0.4294	1.5562	0.8544
$\Delta\delta V_{z_E}$(cm/s)	0.4717	1.2229	0.5206
$\Delta\psi_1$ (deg)	0.0856	0.8445	0.2093
$\Delta\psi_2$ (deg)	0.1175	0.6421	0.2186
$\Delta\psi_3$ (deg)	0.1101	1.1686	0.3306

(b) large lever-arm vector difference

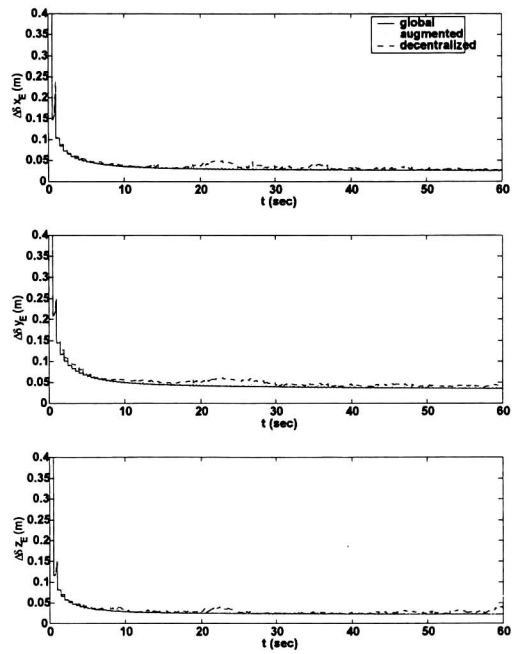

(a) relative position error covariances

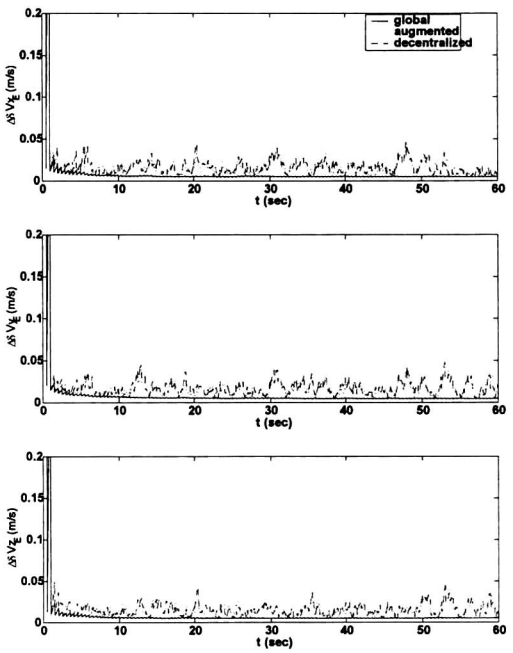

(b) relative velocity error covariances

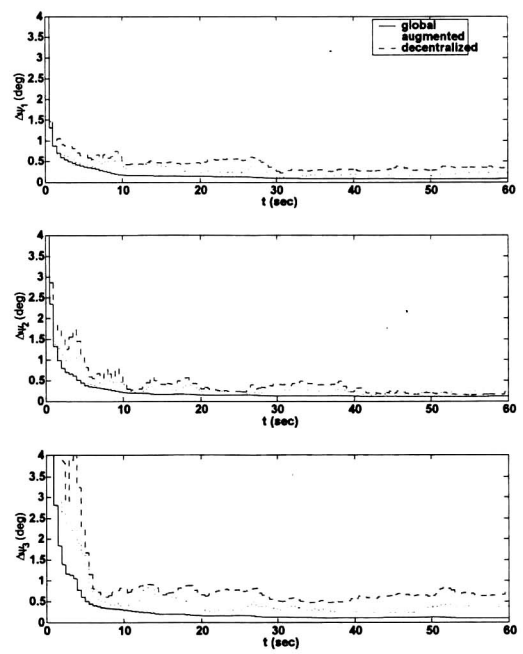

(c) relative attitude error covariances

Fig. 1. No lever-arm vector difference

The first case corresponds to the best situation, $\Delta A \approx 0$ and $\Delta H \approx 0$. On the other hand, the worst lever-arm vector difference of the second case induces nonzero values of ΔH. The same nominal trajectories are employed in both cases.

Table 1(a) represents the relative error covariances of the first case, no lever-arm vector difference, at t_f=60 sec. *Global, Decentralized,* and *Augmented* denote the results of the global filter, the decentralized filter, and the augmented decentralized filter, respectively. The error covariances specified in the table are their square root value. The slight superiority of the performance of the global filter results from the fact that it considers nonzero ΔA and ΔH. The different turbulence effect on each aircraft induces the slight nonzero values. The performance of the augmented decentralized filter is less degraded than that of the decentralized filter. Fig. 1 illustrates the time histories of the square roots of the error covariances. Although the performance of the decentralized filter is acceptable, it is observed that it is more sensitive to the nonzero values than the augmented filter.

The results of the second case (large lever-arm vector difference) are represented in Table 1(b) and Fig. 2. The large ΔH induces the more degraded performance in the decentralized filter

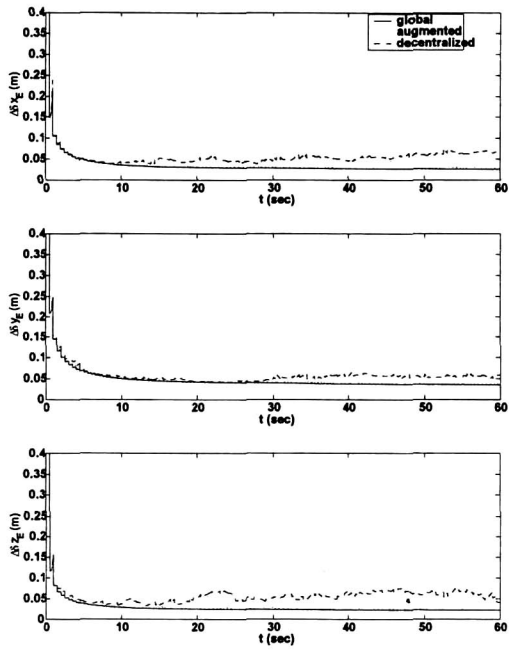

(a) relative position error covariances

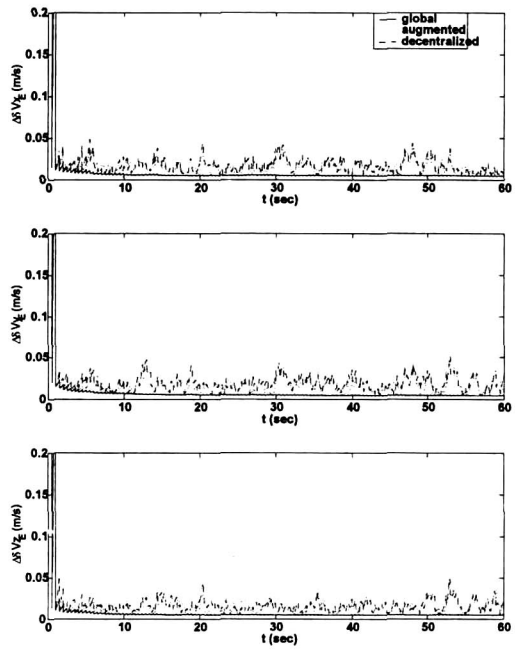

(b) relative velocity error covariances

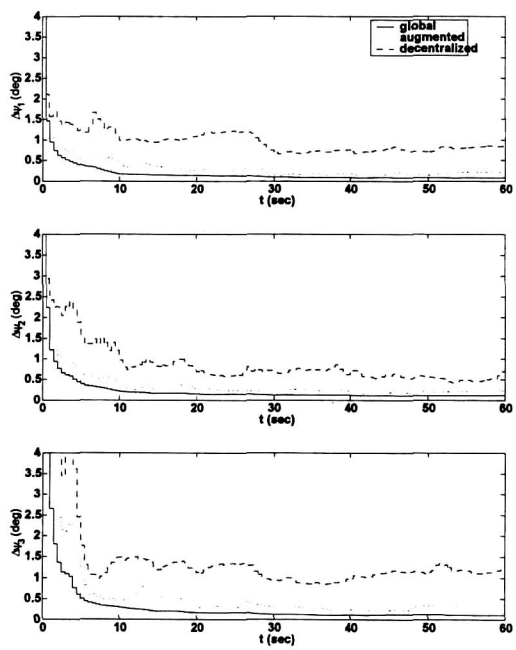

(c) relative attitude error covariances

Fig. 2. Large lever-arm vector difference

when compared with the 1st case in Table 1(a). Fig. 2(a) shows that the relative position error covariances even diverge. Although the final errors at 60 sec are small, it is clear that the invalid assumptions degrade the accuracy. On the other hand, the difference between the augmented filter and the global filter is quite small. The values of the augmented filter in Table 1(b) are not larger than those in Table 1(a). Also the results illustrated in Fig. 2 are similar to those in Fig. 1. These results support the fact that the augmentation of the measurements noise covariance as suggested here compensates the modeling errors of the decentralized filter well.

Concluding Remarks

The relative dynamics obtained to cancel the common-mode noises of GPS measurements still have some terms related to the absolute error states. They act as a main source of filtering errors in the situation that different lever-arm vectors between formation vehicles are employed. An approach of transmitting the covariance of these terms from the base vehicle to the slave vehicle is suggested to compensate the error. Although it is an ad-hoc technique in the sense

that there is no strict proof of its optimality, its superiority is established numerically by the covariance analysis; Its resultant estimation accuracy is very close to the global optimum and exceeds that of existent decentralized filters. Also it does not need the huge computational and communicational burdens of the global filter. For the complete investigation of the proposed filter performance, more elaborate analysis tool will be considered in the near future.

Acknowledgement

This work was supported by postdoctral fellowships program from Korea Science & Engineering Foundation (KOSEF).

References

1. Hummel, D., 1996, "The use of aircraft wakes to achieve power reduction in formation flight," *Advisory Group for Aerospace Research and Development*, AGARD-CP-584, 7 Rue Ancelle, 92200 Neuilly-Sur-Seine, France.

2. Chichka, D. and Speyer, J., 1998, "Solar-powered, formation-enhanced aerial vehicle systems for sustained endurance," *Proceedings of the American Control Conference*, Philadelphia, PA, pp. 684-688.

3. Buechler, D. and Foss, M., 1987, "Integration of GPS and Strapdown inertial subsystems into a single unit," *Journal of The Institute of Navigation*, Vol. 34, No. 2, pp. 140-159.

4. Tazartes, D. A. and Mark, J. G., 1988, "Integration of GPS receivers into existing inertial navigation systems," *Journal of the Institute of Navigation*, Vol. 35, No. 1, pp. 105-119.

5. Johannessen, R. and Asbury, M. J., 1991, "Towards a quantitative assessment of benefits INS/GPS integration can offer to civil aviation," *Journal of the Institute of Navigation*, Vol. 37, No. 4, pp. 329-346.

6. Carvalho, H., Moral, P. D., Monin, A., and Salut, G., 1997, "Optimal nonlinear filtering in GPS/INS integration," *IEEE Trans. Aerospace and Electronic Systems*, Vol. 33, No. 3, pp. 835-849.

7. Farrell, J. A., Givargis, T., and Barth, M., 1999, "Differential carrier phase GPS-Aided INS for automotive applications," *Proceedings of the American Control Conference*, pp. 3660-3664.

8. Olsen, E. A., Park, C. W., and How, J. P., 1999, "3D formation flight using differential carrier-phase GPS sensors," *Journal of Institute of Navigation*, Vol. 46, No. 1, pp. 35-48.

9. Williamson, W., Min, J., Speyer, J. L., and Farrell, J., 1999, "A comparison of state space, range space, and carrier phase differential GPS/INS relative navigation," *Proceedings of the American Control Conference*, Chicago, Illinois, pp. 2932-2938.

10. Williamson, W., Rios, T., and Speyer, J. L., 1999, "Carrier phase differential GPS/INS positioning for formation flight," *Proceedings of the American Control Conference*, San Diego, California, pp. 3665-3670.

11. *Ashtech Z-Surveyor Operation and Reference Manuals*, 1997, Ashtech Corporation, Sunnyvale, CA.

12. Speyer, J. L., 1979, "Computation and transmission requirements for a decentralized linear-quadratic-Gaussian control problem," *IEEE Trans. Automatic Control*, AC-24, pp. 266-269.

13. Chang, T. S., 1980, "Comments on 'Computation and transmission requirements for a decentralized linear-quadratic-Gaussian control problem'," *IEEE Trans. Automatic Control*, AC-25, pp. 609-610.

14. Willsky, A. S., Bello, M. G., Castanon, D. A., Levy, B. C., and Verghese, G. C., 1982, "Combining and updating of local estimates and regional maps along sets of one-dimensional tracks," *IEEE Trans. Automatic Control*, AC-27, pp. 799-813.

15. Castanon, D. A., and Teneketzis, D., 1985, "Distributed estimation algorithm for nonlinear systems," *IEEE Trans. Automatic Control*, AC-30, pp. 418-425.

16. Carlson, N. A., 1990, "Federated square root filter for decentralized parallel processes," *IEEE Trans. Aerospace and Electronic Systems*, Vol. 26, pp. 517-525.

17. Roy, S. and Iltis, R. A., 1991, "Decentralized linear estimation in correlated measurement noise," *IEEE Trans. Aerospace and Electronic Systems*, Vol. 27, pp. 939-941.

18. Wei, M. and Schwarz, K. P., 1990, "A strapdown inertial algorithm using an earth-fixed cartesian frame," *Navigation*, Vol. 37, No. 2, pp. 153-167.

19. Siouris, G. M., 1993, *Aerospace Avionics Systems: A Modern Synthesis.*, Academic Press, Inc.

20. Farrell, J. A. and Barth, M., 1999, *The Global Positioning System & Inertial Navigation*, McGraw-Hill.

21. Maybeck, P. S., 1979, *Stochastic Models, Estimation, and Control,* Academic Press, Vol. 1.

22. Maybeck, P. S., 1982, *Stochastic Models, Estimation, and Control*, Academic Press, Vol. 2.

23. Mclean, D., 1990, *Automatic Flight Control Systems,* Prentice Hall International Series in Systems and Control Engineering, Englewood Cliffs, NJ.